

EVALUATION OF SEISMIC PERFORMANCE OF WOODEN HOUSES WITH SLIDING BASE BY FULL-SCALE SHAKING TABLE TEST

Ai Tomita¹, Yuji Miyazu², Takehiro Wakita³, Takaki Tojo⁴, Takashi Aoki⁵, Masayuki Nagano⁶

ABSTRACT: For the purpose of validating the effectiveness of the sliding base for reducing the seismic response, we first conducted a shaking table test of a full-scale two-story wooden frame. In addition, we also propose an evaluation formula for the coefficient of friction and confirm its effectiveness through a time history response analysis that simulates the test results using the calculated friction coefficient. The test results show that the sliding base reduces the maximum story drift angle to 1/100 rad or less even for the input of ground motion that causes severe damage to conventional wooden houses. The analysis results indicated that the test results could be simulated by the time history response analysis using the friction coefficient calculated by the proposed evaluation formula of the friction coefficient.

KEYWORDS: Sliding base, Friction, Contact-pressure, Wooden house, Shaking table test

1 INTRODUCTION

Although research and development of seismic isolation and vibration control technology are being promoted as a method of improving the seismic performance of detached wooden houses, seismic isolation technology is not sufficiently widespread mainly because the installed cost is high. To resolve this situation, a sliding base that can be introduced at low cost has been proposed by Soda [1]. Previous studies have demonstrated the effectiveness of sliding base in reducing seismic response [2] [3]. However, full-scale shaking table test for two-story wooden frame has not yet been conducted. Therefore, in this paper, we conducted full-scale shaking table test of two-story wooden frame assuming a wooden house with standard specifications and examined the behaviour of the sliding base and the seismic response of the superstructure. We also propose an evaluation formula for the coefficient of friction and verify its validity by performing a time history response analysis that simulates the test results using the calculated friction coefficient.

2 OVERVIEW OF SLIDING BASE STRUCTURE

Figure 1 depicts the outline of the sliding base structure. The sliding base is a structure in which a sliding material is inserted between the reinforced concrete (RC) base and the base concrete. Subjected to a severe earthquake ground motion, the superstructure slides on the sliding material to reduce the seismic force acting on the superstructure.

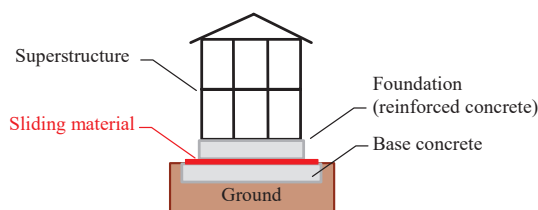


Figure 1: Overview of sliding base structure.

3 SHAKING TABLE TEST

3.1 OVERVIEW OF SHAKING TABLE TEST

Figure 2 shows the two-story wooden frame mounted on the shaking table installed in National Research Institute for Earth Science and Disaster Resilience (NIED), in Tsukuba, Japan. Figure 3 shows the elevation of both test frames, and Figure 4 shows the plan of each floor. There were two types of the base: Fixed Base (FB) [4] and Sliding Base (SB). Steel plate weights were installed on the second and the roof so that the mass of the superstructure was 2.61 t on the second floor and 1.73 t on the roof for both. The mass of the RC base of the SB was 6.81 t. There were two types of seismic elements: a 45×90 mm X-shaped brace wall and a structural plywood wall made by connecting 12 mm structural plywood with CN50 nails at a pitch of 150 mm. Figure 5 and Table 1 displays the details of the sliding base and the sliding materials. The base of the sliding base was an RC structure. A fluororesin sheet and a rubber mat as a protective material were laid between the RC base and the base concrete. The base concrete was fixed on the shaking

¹ Ai Tomita, JSPS Research Fellow, (Doctoral Student, Tokyo University of Science), 7121706@ed.tus.ac.jp

² Yuji Miyazu, Associate Professor, Tokyo University of Science, Dr. Eng., miyazu@rs.tus.ac.jp

³ Takehiro Wakita, Guest Associate Professor, Waseda University, Dr. Eng., t.wakita@aoni.waseda.jp

⁴ Takaki Tojo, R&D Institute, Takenaka Corporation, toujou.takaki@takenaka.co.jp

⁵ Takashi Aoki, National Research Institute for Earth Science and Disaster Resilience (NIED), Dr. Eng., taoki@bosai.go.jp

⁶ Masayuki Nagano, Professor, Tokyo University of Science, Dr. Eng., nagano-m@rs.tus.ac.jp

table around four circumferences using steel jigs. In order to constrain the in-plane rotation of the RC base during excitation, a guide rail was installed along the excitation direction on the side of the RC base. In order to reduce the frictional force generated by the contact between the guide rail and the RC base, a polypropylene sheet and a fluororesin sheet were inserted on the contact surface. In the FB, the base was fixed to the H-shaped steel with anchor bolts, and the H-shaped steel was fixed to the shaking table. The first-mode natural period of the

superstructure under micro-vibration, which was evaluated by excitation using white noise, was 0.16 seconds for the FB and 0.19 seconds for the SB. Table 2 displays the information of input ground accelerations. An artificially synthesized motion 1 and 2 are the middle- and the large-scale earthquake ground motions defined in the Japanese Building Standards Act, respectively. The time history and pseudo velocity response spectrum of the input ground accelerations are shown in Figures 6 and 7.

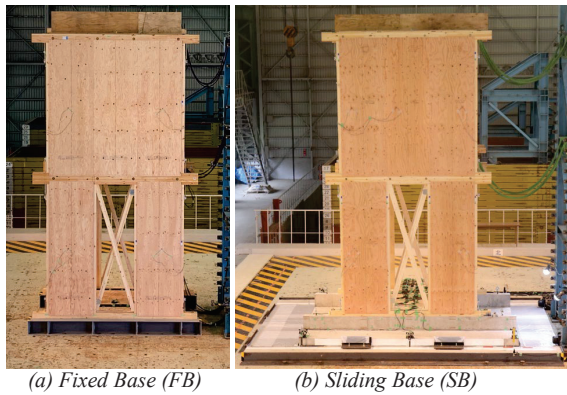


Figure 2: The photograph of the test frames.

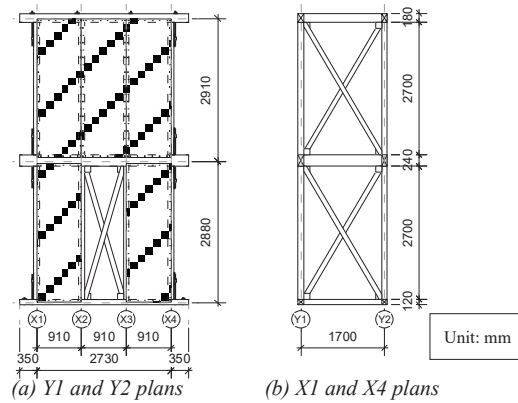


Figure 3: Elevation of the wooden frame.

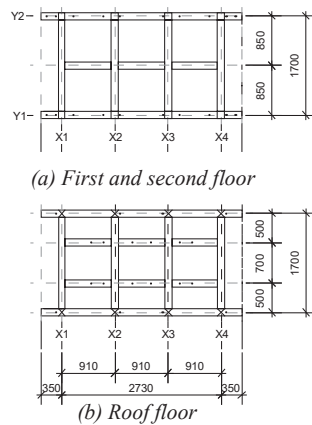


Figure 4: Plan of the wooden frame.

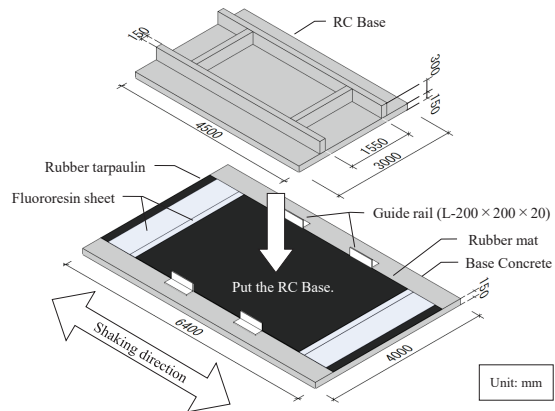


Figure 5: Detail of the sliding base.

Table 1: Materials used for sliding base.

Sliding material (material thickness)	Use applications
Rubber mat (t = 5 mm)	Installed on the sliding material as a protective material for the upper sliding material
Fluororesin sheet (t = 0.2 mm)	Installed between a rubber tarpaulin and a rubber mat as a lower and upper sliding material
Rubber tarpaulin (t = 2 mm)	Installed on the base concrete as a protective material for the lower sliding material

Table 2: Input ground accelerations.

Name	(Abbreviation)	Maximum acceleration (m/s ²)
Artificially Synthesized Motion 1 50%	(BCJ_Lv1*0.5)	1.04
Artificially Synthesized Motion 1 100%	(BCJ_Lv1)	2.07
Artificially Synthesized Motion 2 100%	(BCJ_Lv2)	3.56
2016 Kumamoto earthquake, KiK-net Mashiki Foreshock EW 75%	(MSKf*0.75)	6.94
2016 Kumamoto earthquake, KiK-net Mashiki Mainshock EW 75%	(MSKm*0.75)	8.68
1995 Kobe earthquake, JMA Kobe NS 100%	(KOBE)	8.18

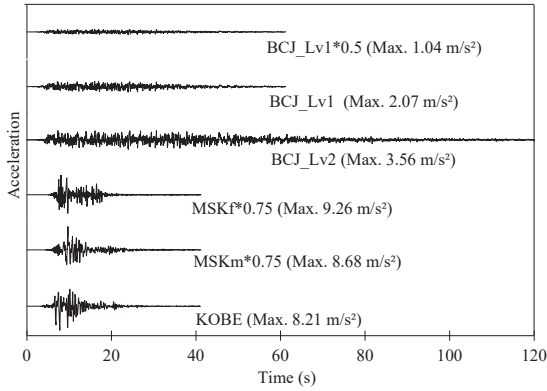


Figure 6: Time history of the input ground accelerations.

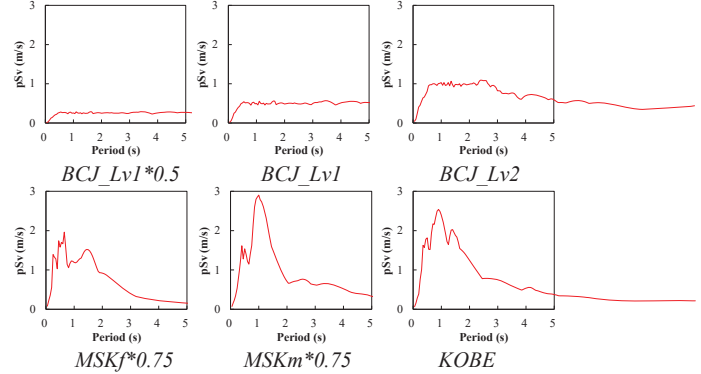


Figure 7: Pseudo velocity response spectra ($h=5\%$) of the observed wave on the shaking table.

3.2 CALCULATION METHOD OF THE FRICTION COEFFICIENT

Equation (1) shows the calculation method of the friction coefficient when the cumulative dissipated energy is equivalent, and the vertical ground motion is taken into consideration. The sign of the denominator in Equation (1) is the same as the sign of the slip velocity V defined in Equation (2).

$$\bar{\mu} = \frac{\sum_{t=0}^T (N_{t+\Delta t} + N_t) (L_{t+\Delta t} - L_t)}{\sum_{t=0}^T \pm m(2g + a_{t+\Delta t} + a_t) (L_{t+\Delta t} - L_t)} \quad (1)$$

$$V = \frac{L_{t+\Delta t} - L_t}{\Delta t} = \frac{\Delta L_t}{\Delta t} \quad (2)$$

where N_t is friction force of the sliding surface at time t , L_t is the sliding displacement at time t , a_t is vertical response acceleration of the sliding base at time t , T is earthquake duration, m is total mass of the structure and g is gravitational acceleration.

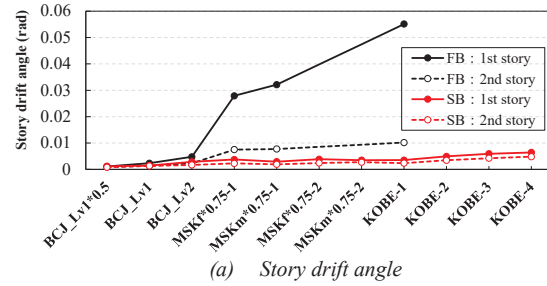
In order to eliminate the influence of noise contained in the measurement data, the sliding displacement L_t was subjected to moving average processing with an average interval of 0.02 seconds. In addition, when the value of ΔL_t is less than the threshold shown in Table 3, it was assumed that no sliding occurred during Δt ($\Delta L_t = 0$). The threshold was set for each excitation to be slightly larger than ΔL_t before the start of excitation.

Table 3: Threshold for calculation of coefficient of friction.

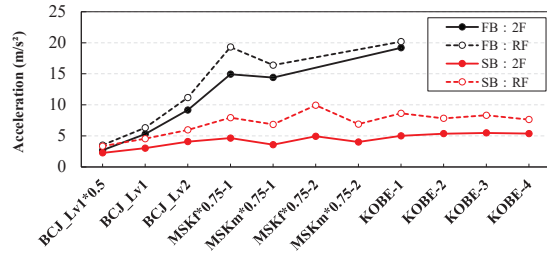
Name	Threshold (mm)
BCJ_Lv2	0.10
MSKf*0.75, MSKm*0.75, KOBE	0.20

3.3 TEST RESULTS

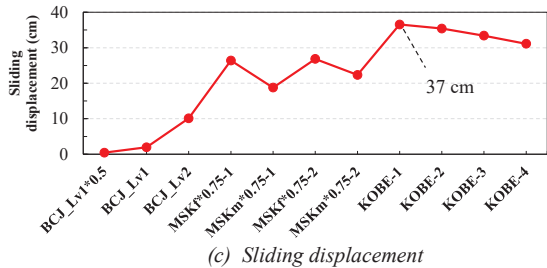
Figure 8 compares the maximum response for each input ground acceleration. In the FB, first story drift angle of MSKf*0.75-1 increased sharply, and first story drift angle of KOBE-1 further increased. Whereas in the SB, the



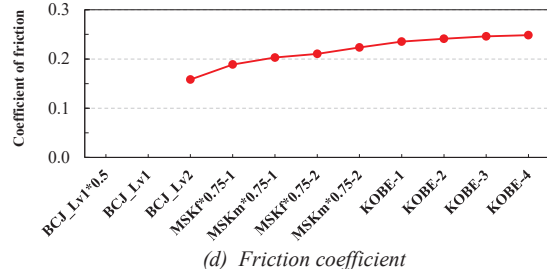
(a) Story drift angle



(b) Acceleration



(c) Sliding displacement



(d) Friction coefficient

Figure 8: Maximum response of FB and SB for each input ground acceleration.

maximum story drift angle is reduced to 1/100 rad or less in all excitations. It is seen that the maximum response acceleration of each floor is also reduced by the sliding base. The maximum sliding displacement was 37 cm at KOBE-1. It can be seen that the coefficient of friction gradually increases with repeated excitation. In addition, it is found that the maximum sliding displacement decreases as the friction coefficient increases due to repeated excitation of KOBE. Figure 9 shows the values obtained by dividing the response values of the SB by those of the FB. By using a sliding base, it is possible to reduce the response, especially against strong ground motions. The maximum story drift angle of the first story was reduced to 13% with excitation of MSKf*0.75-1, 10% with excitation of MSKm*0.75-1, and 8% with excitation of KOBE-1. The maximum response acceleration on the second floor was reduced by 25% with excitation of MSKm*0.75-1, and the maximum response acceleration on the roof floor was reduced to about 40% by excitation of MSKf*0.75-1 to KOBE-1. From the acceleration response spectra on the first and second floors shown in Figures 10 and 11, it can be seen that the frequency characteristics have changed and the response value has been reduced by applying the sliding base. Figure 12 shows the force deformation relations of each story of the FB and the SB. It can be seen that the maximum force of first story can be reduced to about half by applying the sliding base.

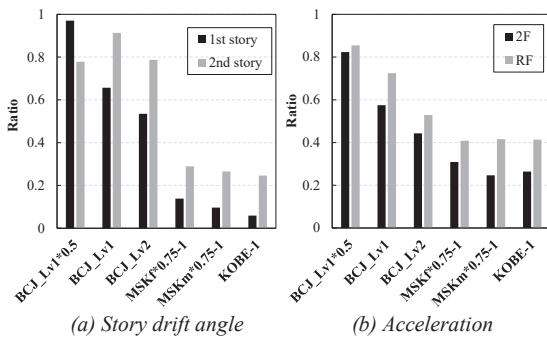


Figure 9: Ratio of the response of SB to that of FB.

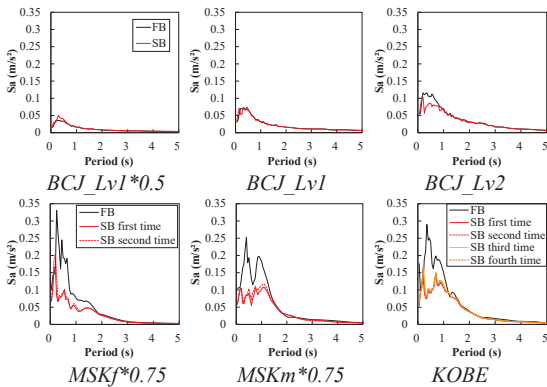


Figure 10: Acceleration response spectra ($h=5\%$) of the observed wave on the first floor.

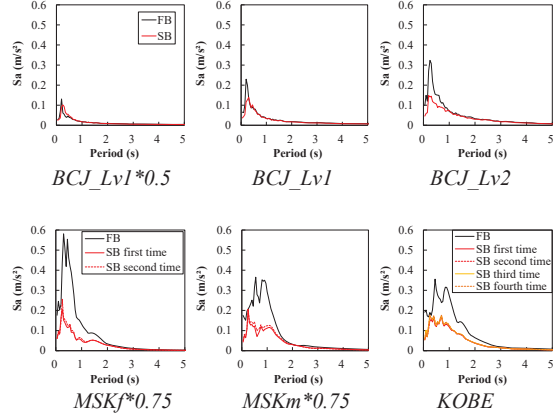


Figure 11: Acceleration response spectra ($h=5\%$) of the observed wave on the second floor.

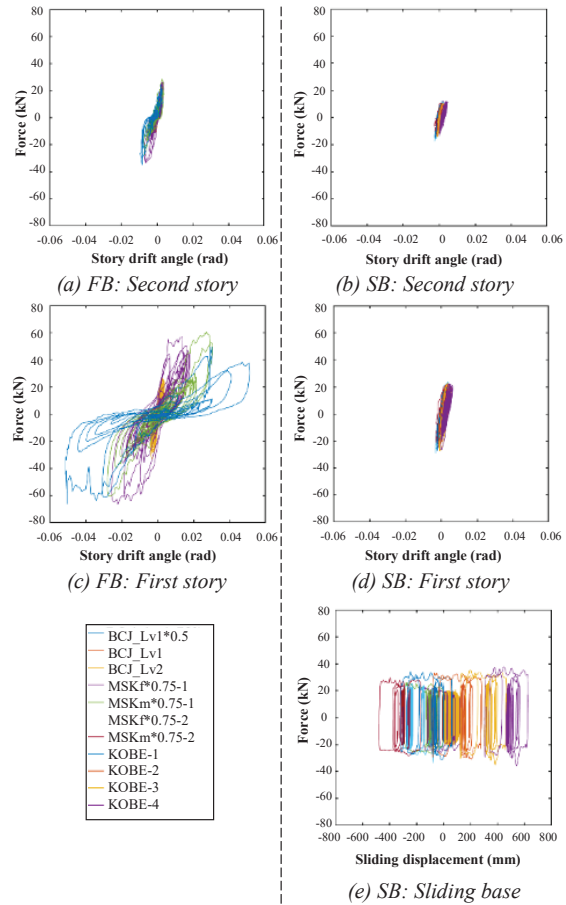


Figure 12: Force-deformation relations of FB and SB.

Time history of the sliding displacement, the story drift angle and the acceleration of the FB and the SB are compared in Figures 13 (a), (b) and (c), respectively. It can be seen that the base of the SB moved mainly in one direction and finally stopped with the residual displacement of about 20 cm. The residual displacement highly depends on the characteristic of the input ground motion; however, it is important to take it into

consideration at the design stage of the building with the sliding base. It can be confirmed in Figures 13 (b) and (c) that the story drift of the SB is lower than that of the FB in all the time, whereas the acceleration is reduced mainly during from 12 to 14 s and during from 15 to 16 s when the sliding of the base occurred.

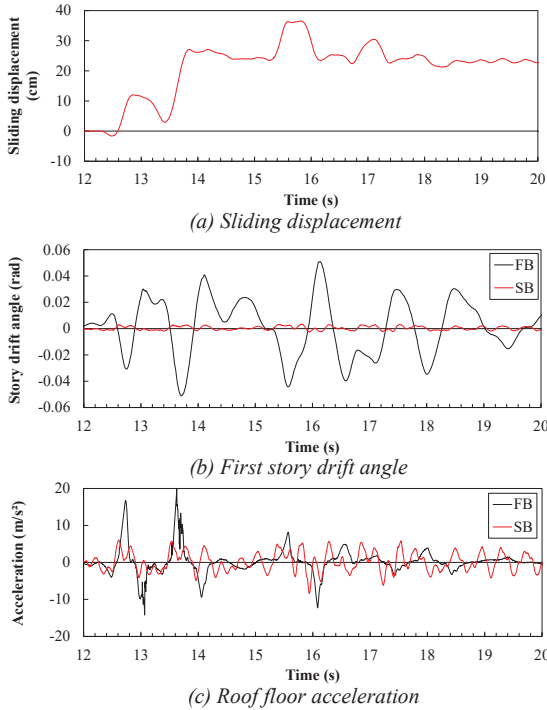


Figure 13: Time histories when input KOBE-1.

The damage condition of the sliding material after all shakings is shown in Figure 14. It was confirmed that the sliding material was torn by about 1.3m after the end of all excitations. Considering this together with the results of maximum response, at least the increase in the friction coefficient and the decrease in the maximum sliding displacement after KOBE-2 can be attributed to damage to the sliding material.

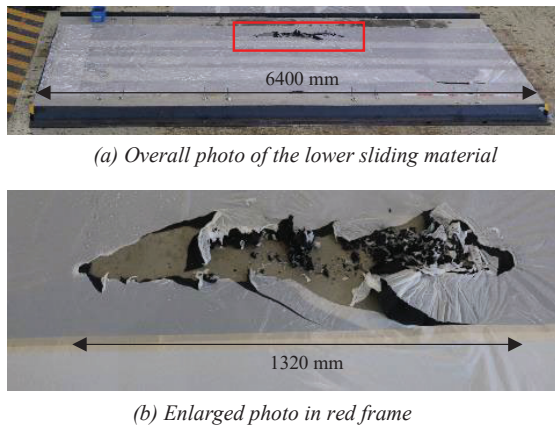


Figure 14: The photograph of the damage condition of the sliding material after full excitation.

4 TIME HISTORY SEISMIC RESPONSE ANALYSIS

4.1 OVERVIEW OF ANALYSIS

Each test frame was model in the multi-mass shear system depicted in Figure 15, and the simulation of the experiment was performed by time history response analysis. The mass of each floor was 6.81 t for the sliding base, 2.61 t for the second floor, and 1.73 t for the roof floor. An elastic-perfectly plastic model was used to model the sliding base. The yield force of the elastic-perfectly plastic model was obtained by multiplying the friction coefficient estimated from the test results by the total mass of the SB, 10.84 t. The coefficient of friction was set to 0.197, which is the average value from BCJ_Lv2 to MSKm*0.75-2, taking into account the effect of repetition. The initial stiffness of the elastic-perfectly plastic model was set to reach the yield force at 0.01 mm deformation. For the modelling of the superstructure, we used the ENCL model [5], which simulates the force deformation relations obtained from cyclic loading test on structural plywood walls and X-shaped brace walls. Figure 16 shows the force deformation relations of the ENCL model. The ENCL model for four structural plywood walls and the ENCL model for two X-shaped brace walls were placed in parallel on the first story, and the ENCL model for six structural plywood walls was installed on the second story. The damping of the superstructure was set to 1% of the initial stiffness proportional type, and no viscous damping was applied to the sliding base. The natural periods of the first mode of the FB and the SB are 0.282 s and 0.284, respectively. The input seismic motion was the acceleration measured on the shaking table, and the input acceleration was set to 0 between each excitation for 10 seconds, so that the free vibration after the excitation was sufficiently damped. OpenSees [6] was used to perform the time history analysis, and the Newmark β ($\beta = 0.25$) was used for the numerical integration. The step time of the calculation was 1/10000 seconds.

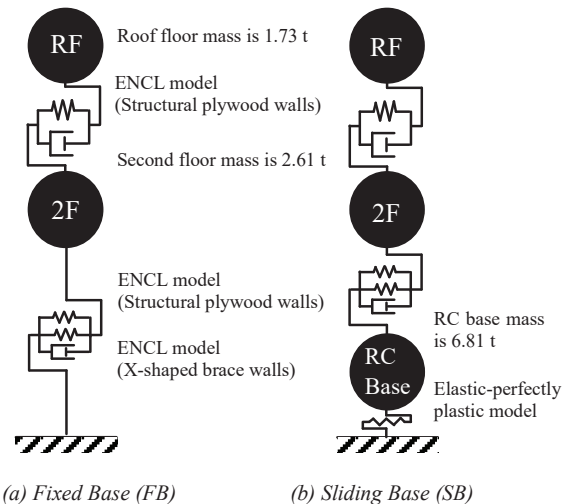


Figure 15: The analysis model of FB and SB.

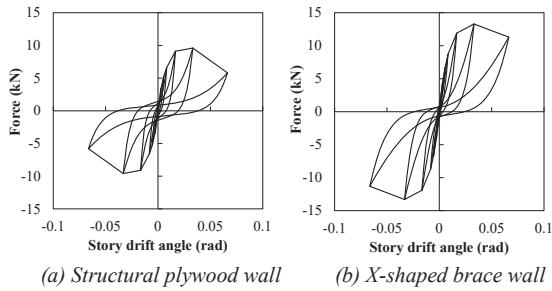


Figure 16: Force-deformation relations of seismic walls.

4.2 NUMERICAL ANALYSIS RESULTS

Figure 17 shows a comparison of the test results and analysis results for the FB, and Figure 18 shows a comparison of the test results and the analysis results for the SB. In the FB, the maximum story drift angle of the second story agree well with the test results. On the other hand, the analysis results for the first story were larger with excitation up to BCJ_Lv2, and smaller with excitation after the MSK*0.75-1. Regarding the maximum response acceleration, the test results can be simulated on the second floor and the roof floor with the excitation up to MSK*0.75-1. The maximum sliding displacement of the SB model generally simulates the test results. The maximum story drift angle is almost the same as the test results for the second story, but for the first story, there is a difference between the test results and the analysis results. As for the maximum response acceleration, the analysis results are excessive for both the second floor and the roof floor.

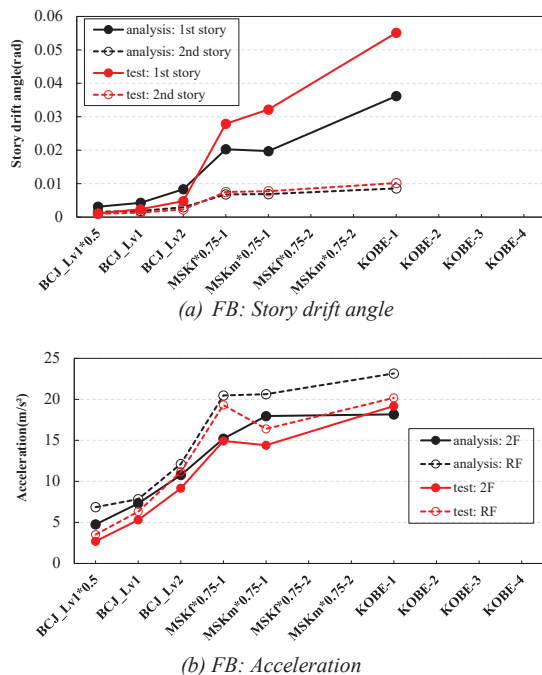
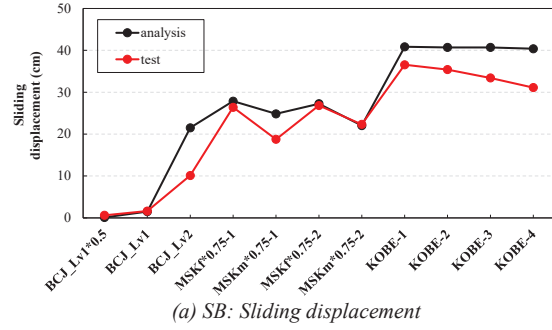
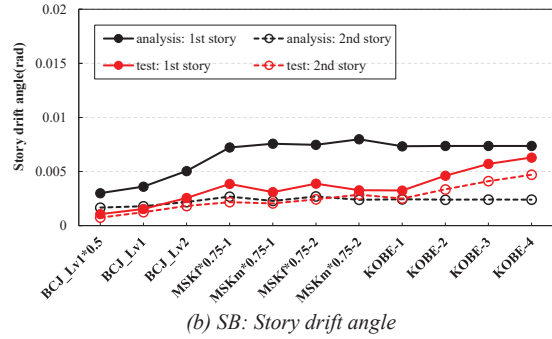


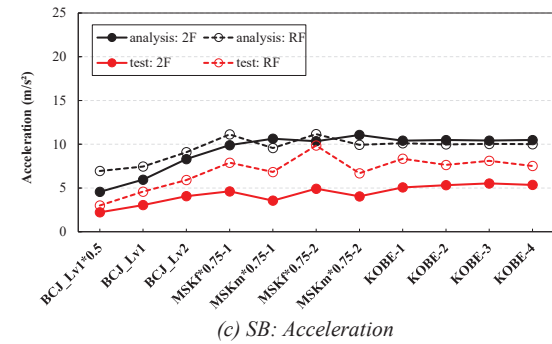
Figure 17: Maximum response of analysis and test (FB).



(a) SB: Sliding displacement



(b) SB: Story drift angle



(c) SB: Acceleration

Figure 18: Maximum response of analysis and test (SB).

Figure 19 compares the force-deformation relation between test and analysis results. In the test, the considerable degradation of the resistance occurred due to the buckling failure of the brace wall, which is not considered in the analysis model. It can be seen that both the maximum deformation and the maximum force of the superstructure of the SB are larger in the analysis results. From the force deformation relations of the sliding base, it can be seen that the difference in cumulative sliding displacement is large. Summarizing the maximum response results, the following two points are considered to be the factors for the difference between the analysis results and the experimental results. (1) Set low stiffness and yield strength of the analytical model in the small deformation region below about 1/100 rad. (2) In the region of large deformation above 1/30 rad, the analytical model does not consider the significant reduction of resistance due to the buckling failure of braces.

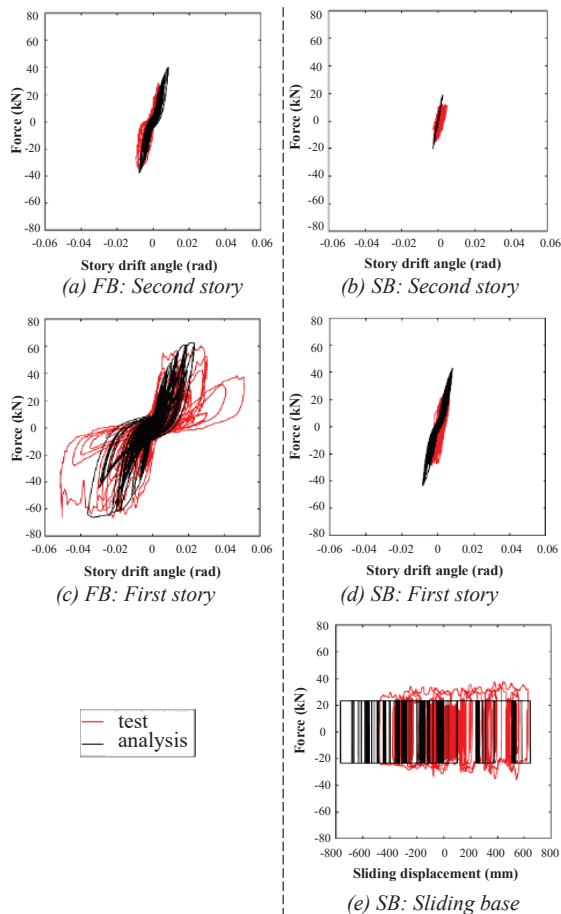


Figure 19: Force-deformation relations of test and analysis.

5 CONCLUSIONS

In order to understand the seismic response characteristics of a full-scale two-story wooden frame to which a sliding base is applied, a full-scale shaking table test and time history response analysis were carried out.

- 1) It is confirmed through the shaking table test that the maximum story drift angle can be reduced to 1/100 rad or less even under extremely strong ground motion by the applying of the sliding base. The maximum sliding displacement of the sliding base was about 37 cm for the input of KOBE-1.
- 2) In the analytical study, even with a simple mass-shear system model in which the sliding base is represented by an elastic perfect plastic model, the analysis results shows good agreement with the test result. From this, it can be seen that the friction coefficient calculated by the proposed evaluation formula is appropriate.

ACKNOWLEDGEMENT

This work was supported by the grant from the Japan Society for the Promotion of Science (JSPS KAKENHI

Grant Number JP 22J12689) and the Japan Society of Seismic Isolation (JSSI).

REFERENCES

- [1] S. Soda, Y. Miyazu: SEISMIC RESPONSE CONTROL OF WOODEN HOUSE PLACED ON SLIDING BASE, Proceedings of the 9th U.S. National and 10th Canadian Conference on Earthquake Engineering, Paper No. 1508, 2010.
- [2] Satsuya SODA, Hirosuke FUJITA, Emi MIYAMOTO: Study on seismic response reduction of building on sliding base by full scale shaking table test, Summaries of Technical Papers of Annual Meeting Architectural Institute of Japan, pp. 623-624, 2009. (in Japanese)
- [3] Hong-Song Hu, Fan Lin, Yi-chao Gao, Zi-Xiong Guo, Chen Wang: Maximum Superstructure Response of Sliding-Base Structures under Earthquake Excitation, J. Struct Eng., 146(7),2020
- [4] T. Katada, Y. Miyazu, S. Kageyama, T. Mori, H. Isoda: Prevention of Soft-Story Mechanism of Wooden Houses Using Continuous Walls., AIJ J. Technol. Des. Vol. 27, No. 67, 1243-1248, 2021. (in Japanese)
- [5] H. Matsunaga, Y. Miyazu, S. Soda: A Universal Modelling Method for Wooden Shear/ Nonshear Walls, Journal of Structural and Construction Engineering, Vol. 74, pp.889-896, 2009. (in Japanese)
- [6] PEER: OpenSees, <http://opensees.berkeley.edu>, reference 2022.